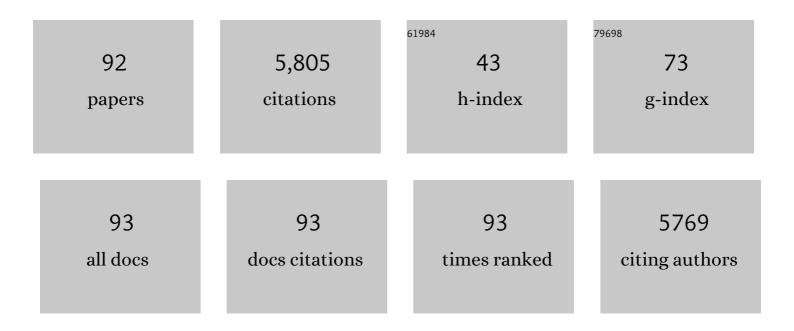
## Jianlu Wang

List of Publications by Year in descending order

Source: https://exaly.com/author-pdf/2580695/publications.pdf Version: 2024-02-01



| #  | Article   | IF   | CITATIONS |
|----|---|------|-----------|
| 1  | Ultrasensitive and Broadband MoS <sub>2</sub> Photodetector Driven by Ferroelectrics. Advanced<br>Materials, 2015, 27, 6575-6581.   | 21.0 | 722       |
| 2  | Unipolar barrier photodetectors based on van der Waals heterostructures. Nature Electronics, 2021,<br>4, 357-363.   | 26.0 | 292       |
| 3  | Recent Progress on Localized Field Enhanced Twoâ€dimensional Material Photodetectors from<br>Ultraviolet—Visible to Infrared. Small, 2017, 13, 1700894.                     | 10.0 | 234       |
| 4  | Arrayed Van Der Waals Broadband Detectors for Dualâ€Band Detection. Advanced Materials, 2017, 29,<br>1604439.   | 21.0 | 218       |
| 5  | Highâ€Performance Photovoltaic Detector Based on MoTe <sub>2</sub> /MoS <sub>2</sub> Van der<br>Waals Heterostructure. Small, 2018, 14, 1703293.                            | 10.0 | 205       |
| 6  | Programmable transition metal dichalcogenide homojunctions controlled by nonvolatile ferroelectric domains. Nature Electronics, 2020, 3, 43-50.                             | 26.0 | 167       |
| 7  | Perpendicular Optical Reversal of the Linear Dichroism and Polarized Photodetection in 2D GeAs. ACS Nano, 2018, 12, 12416-12423.  | 14.6 | 157       |
| 8  | When Nanowires Meet Ultrahigh Ferroelectric Field–High-Performance Full-Depleted Nanowire<br>Photodetectors. Nano Letters, 2016, 16, 2548-2555.                             | 9.1  | 135       |
| 9  | Ultrafast non-volatile flash memory based on van der Waals heterostructures. Nature<br>Nanotechnology, 2021, 16, 874-881.   | 31.5 | 130       |
| 10 | A Robust Artificial Synapse Based on Organic Ferroelectric Polymer. Advanced Electronic Materials, 2019, 5, 1800600.  | 5.1  | 129       |
| 11 | Highâ€5ensitivity Floatingâ€Gate Phototransistors Based on WS <sub>2</sub> and MoS <sub>2</sub> .<br>Advanced Functional Materials, 2016, 26, 6084-6090.                    | 14.9 | 124       |
| 12 | Ultrasensitive negative capacitance phototransistors. Nature Communications, 2020, 11, 101.   | 12.8 | 124       |
| 13 | AsP/InSe Van der Waals Tunneling Heterojunctions with Ultrahigh Reverse Rectification Ratio and<br>High Photosensitivity. Advanced Functional Materials, 2019, 29, 1900314. | 14.9 | 121       |
| 14 | Blackbody-sensitive room-temperature infrared photodetectors based on low-dimensional tellurium grown by chemical vapor deposition. Science Advances, 2021, 7, .            | 10.3 | 121       |
| 15 | Recent Progress on Electrical and Optical Manipulations of Perovskite Photodetectors. Advanced Science, 2021, 8, e2100569.  | 11.2 | 118       |
| 16 | MoTe <sub>2</sub> p–n Homojunctions Defined by Ferroelectric Polarization. Advanced Materials,<br>2020, 32, e1907937.   | 21.0 | 115       |
| 17 | Highâ€Performance Ferroelectric Polymer Sideâ€Gated CdS Nanowire Ultraviolet Photodetectors.<br>Advanced Functional Materials, 2016, 26, 7690-7696.                         | 14.9 | 107       |
| 18 | Ferroelectric Negative Capacitance Field Effect Transistor. Advanced Electronic Materials, 2018, 4,<br>1800231.   | 5.1  | 105       |

| #  | Article   | IF   | CITATIONS |
|----|---|------|-----------|
| 19 | Amorphous Gallium Oxideâ€Based Gateâ€Tunable Highâ€Performance Thin Film Phototransistor for<br>Solarâ€Blind Imaging. Advanced Electronic Materials, 2019, 5, 1900389.  | 5.1  | 95        |
| 20 | Logic gates based on neuristors made from two-dimensional materials. Nature Electronics, 2021, 4, 399-404.  | 26.0 | 95        |
| 21 | Highâ€Performance Waferâ€6cale MoS <sub>2</sub> Transistors toward Practical Application. Small, 2018, 14, e1803465.  | 10.0 | 88        |
| 22 | Mechanism of Electric Power Generation from Ionic Droplet Motion on Polymer Supported Graphene.<br>Journal of the American Chemical Society, 2018, 140, 13746-13752.  | 13.7 | 87        |
| 23 | Controlled Doping of Waferâ€Scale PtSe <sub>2</sub> Films for Device Application. Advanced Functional Materials, 2019, 29, 1805614.   | 14.9 | 87        |
| 24 | Ferroelectric Localized Field–Enhanced ZnO Nanosheet Ultraviolet Photodetector with High<br>Sensitivity and Low Dark Current. Small, 2018, 14, e1800492.  | 10.0 | 85        |
| 25 | Ferroelectric-tuned van der Waals heterojunction with band alignment evolution. Nature<br>Communications, 2021, 12, 4030.   | 12.8 | 79        |
| 26 | Two-dimensional negative capacitance transistor with polyvinylidene fluoride-based ferroelectric polymer gating. Npj 2D Materials and Applications, 2017, 1, .  | 7.9  | 77        |
| 27 | Ultra-sensitive polarization-resolved black phosphorus homojunction photodetector defined by ferroelectric domains. Nature Communications, 2022, 13, .  | 12.8 | 77        |
| 28 | Optoelectronic Properties of Few-Layer MoS <sub>2</sub> FET Gated by Ferroelectric Relaxor Polymer.<br>ACS Applied Materials & Interfaces, 2016, 8, 32083-32088.  | 8.0  | 76        |
| 29 | Integration of Highâ€ <i>k</i> Oxide on MoS <sub>2</sub> by Using Ozone Pretreatment for<br>Highâ€Performance MoS <sub>2</sub> Topâ€Gated Transistor with Thicknessâ€Dependent Carrier Scattering<br>Investigation. Small, 2015, 11, 5932-5938. | 10.0 | 74        |
| 30 | Ultralowâ€Power Machine Vision with Selfâ€Powered Sensor Reservoir. Advanced Science, 2022, 9,<br>e2106092.   | 11.2 | 68        |
| 31 | A Dualâ€Gate MoS <sub>2</sub> Photodetector Based on Interface Coupling Effect. Small, 2020, 16, e1904369.  | 10.0 | 65        |
| 32 | Visible to short wavelength infrared In <sub>2</sub> Se <sub>3</sub> -nanoflake photodetector gated by a ferroelectric polymer. Nanotechnology, 2016, 27, 364002.   | 2.6  | 63        |
| 33 | Ultrasensitive Hybrid MoS <sub>2</sub> –ZnCdSe Quantum Dot Photodetectors with High Gain. ACS<br>Applied Materials & Interfaces, 2019, 11, 23667-23672.   | 8.0  | 62        |
| 34 | Ultrabroadband Photodetectors up to 10.6 µm Based on 2D Fe <sub>3</sub> O <sub>4</sub> Nanosheets.<br>Advanced Materials, 2020, 32, e2002237.   | 21.0 | 57        |
| 35 | A versatile photodetector assisted by photovoltaic and bolometric effects. Light: Science and Applications, 2020, 9, 160.   | 16.6 | 56        |
| 36 | Extremely Low Dark Current MoS <sub>2</sub> Photodetector via 2D Halide Perovskite as the<br>Electron Reservoir. Advanced Optical Materials, 2020, 8, 1901402.  | 7.3  | 55        |

| #  | Article   | IF      | CITATIONS |
|----|---|---------|-----------|
| 37 | Multimechanism Synergistic Photodetectors with Ultrabroad Spectrum Response from 375 nm to 10<br>µm. Advanced Science, 2019, 6, 1901050.  | 11.2    | 52        |
| 38 | Direct Polarimetric Image Sensor and Wide Spectral Response Based on Quasiâ€1D<br>Sb <sub>2</sub> S <sub>3</sub> Nanowire. Advanced Functional Materials, 2021, 31, 2006601.  | 14.9    | 52        |
| 39 | Ferroelectric Synaptic Transistor Network for Associative Memory. Advanced Electronic Materials, 2021, 7, 2001276.  | 5.1     | 52        |
| 40 | Ferroelectric polymer tuned two dimensional layered MoTe <sub>2</sub> photodetector. RSC<br>Advances, 2016, 6, 87416-87421.   | 3.6     | 51        |
| 41 | Symmetric Ultrafast Writing and Erasing Speeds in Quasiâ€Nonvolatile Memory via van der Waals<br>Heterostructures. Advanced Materials, 2019, 31, e1808035.  | 21.0    | 50        |
| 42 | HgCdTe/black phosphorus van der Waals heterojunction for high-performance polarization-sensitive midwave infrared photodetector. Science Advances, 2022, 8, eabn1811.   | 10.3    | 50        |
| 43 | Synthetically controlling the optoelectronic properties of<br>dithieno[2,3-d:2′,3′-d′]benzo[1,2-b:4,5-b′]dithiophene-alt-diketopyrrolopyrrole-conjugated polymers<br>efficient solar cells. Journal of Materials Chemistry A, 2014, 2, 15316-15325. | fo110.3 | 46        |
| 44 | Characterization of atomic defects on the photoluminescence in twoâ€dimensional materials using<br>transmission electron microscope. InformaÄnÃ-Materiály, 2019, 1, 85-97.  | 17.3    | 46        |
| 45 | Ultrasensitive Mid-wavelength Infrared Photodetection Based on a Single InAs Nanowire. ACS Nano, 2019, 13, 3492-3499.   | 14.6    | 45        |
| 46 | Highly Sensitive InSb Nanosheets Infrared Photodetector Passivated by Ferroelectric Polymer.<br>Advanced Functional Materials, 2020, 30, 2006156.   | 14.9    | 41        |
| 47 | Eliminating Overerase Behavior by Designing Energy Band in High-Speed Charge-Trap Memory Based on<br>WSe <sub>2</sub> . Small, 2017, 13, 1604128.   | 10.0    | 39        |
| 48 | High-performance lead-free two-dimensional perovskite photo transistors assisted by ferroelectric dielectrics. Journal of Materials Chemistry C, 2018, 6, 12714-12720.  | 5.5     | 39        |
| 49 | High performance top-gated ferroelectric field effect transistors based on two-dimensional ZnO<br>nanosheets. Applied Physics Letters, 2017, 110, .   | 3.3     | 34        |
| 50 | Ferroelectric Enhanced Performance of a GeSn/Ge Dual-Nanowire Photodetector. Nano Letters, 2020,<br>20, 3872-3879.  | 9.1     | 33        |
| 51 | Complementary Logic with Voltage Zero‣oss and Nanoâ€Watt Power via Configurable<br>MoS <sub>2</sub> /WSe <sub>2</sub> Gate. Advanced Functional Materials, 2018, 28, 1805171.   | 14.9    | 32        |
| 52 | Efficient two-terminal artificial synapse based on a network of functionalized conducting polymer nanowires. Journal of Materials Chemistry C, 2019, 7, 9933-9938.  | 5.5     | 32        |
| 53 | Gateâ€Tunable Photodiodes Based on Mixedâ€Dimensional Te/MoTe <sub>2</sub> Van der Waals<br>Heterojunctions. Advanced Electronic Materials, 2021, 7, 2001066.   | 5.1     | 29        |
| 54 | Ultrahighâ€Detectivity Photodetectors with Van der Waals Epitaxial CdTe Singleâ€Crystalline Films.<br>Small, 2019, 15, e1900236.  | 10.0    | 27        |

| #  | Article   | IF   | CITATIONS |
|----|---|------|-----------|
| 55 | High Performance Ternary Organic Phototransistors with Photoresponse up to 2600 nm at Room<br>Temperature. Advanced Functional Materials, 2021, 31, 2103787.  | 14.9 | 26        |
| 56 | Spatial and Frequency Selective Plasmonic Metasurface for Long Wavelength Infrared Spectral<br>Region. Advanced Optical Materials, 2018, 6, 1800337.  | 7.3  | 23        |
| 57 | Multifunctional MoS <sub>2</sub> Transistors with Electrolyte Gel Gating. Small, 2020, 16, e2000420.  | 10.0 | 23        |
| 58 | MoS <sub>2</sub> /HfO <sub>2</sub> /Siliconâ€Onâ€Insulator Dualâ€Photogating Transistor with Ambipolar<br>Photoresponsivity for Highâ€Resolution Light Wavelength Detection. Advanced Functional Materials,<br>2019, 29, 1906242.             | 14.9 | 22        |
| 59 | Flexible graphene field effect transistor with ferroelectric polymer gate. Optical and Quantum<br>Electronics, 2016, 48, 1.   | 3.3  | 21        |
| 60 | Polarizer-free polarimetric image sensor through anisotropic two-dimensional GeSe. Science China<br>Materials, 2021, 64, 1230-1237.   | 6.3  | 21        |
| 61 | Gate Stack Engineering in MoS <sub>2</sub> Fieldâ€Effect Transistor for Reduced Channel Doping and<br>Hysteresis Effect. Advanced Electronic Materials, 2021, 7, 2000395.   | 5.1  | 19        |
| 62 | Ferroelectric tunnel junctions with high tunnelling electroresistance. Nature Electronics, 2020, 3, 440-441.  | 26.0 | 18        |
| 63 | Electrical characterization of MoS2 field-effect transistors with different dielectric polymer gate.<br>AIP Advances, 2017, 7, .  | 1.3  | 15        |
| 64 | Visualizing Band Profiles of Gate-Tunable Junctions in MoS <sub>2</sub> /WSe <sub>2</sub><br>Heterostructure Transistors. ACS Nano, 2021, 15, 16314-16321.  | 14.6 | 14        |
| 65 | End-Bonded Contacts of Tellurium Transistors. ACS Applied Materials & Interfaces, 2021, 13, 7766-7772.  | 8.0  | 12        |
| 66 | Stable Hysteresis-Free MoS <sub>2</sub> Transistors With Low-k/High-k Bilayer Gate Dielectrics. IEEE<br>Electron Device Letters, 2020, 41, 1036-1039.   | 3.9  | 10        |
| 67 | Two-dimensional series connected photovoltaic cells defined by ferroelectric domains. Applied Physics Letters, 2020, 116, .   | 3.3  | 10        |
| 68 | Interface engineering of ferroelectric-gated MoS2 phototransistor. Science China Information Sciences, 2021, 64, 1.   | 4.3  | 10        |
| 69 | High-Performance Photodetectors with an Ultrahigh Photoswitching Ratio and a Very Fast Response<br>Speed in Self-Powered Cu <sub>2</sub> ZnSnS <sub>4</sub> /CdS PN Heterojunctions. ACS Applied<br>Electronic Materials, 2021, 3, 4135-4143. | 4.3  | 10        |
| 70 | Ferroelectric control of magnetism in P(VDF–TrFE)/Co heterostructure. Journal of Materials Science:<br>Materials in Electronics, 2015, 26, 7502-7506.   | 2.2  | 9         |
| 71 | Ferroelectric properties of gradient doped Y2O3:HfO2 thin films grown by pulsed laser deposition.<br>Applied Physics Letters, 2019, 115, .  | 3.3  | 9         |
| 72 | Ferroelectricity and antiferromagnetism in organic–inorganic hybrid<br>(1,4-bis(imidazol-1-ylmethyl)benzene)CuCl <sub>4</sub> A·H <sub>2</sub> O. CrystEngComm, 2020, 22,<br>587-592.   | 2.6  | 9         |

| #  | Article   | IF         | CITATIONS    |
|----|---|------------|--------------|
| 73 | Ferroelectric field-effect transistors for logic and <i>in-situ</i> memory applications.<br>Nanotechnology, 2020, 31, 424007.   | 2.6        | 9            |
| 74 | Photodetectors: Ultrasensitive and Broadband MoS <sub>2</sub> Photodetector Driven by Ferroelectrics (Adv. Mater. 42/2015). Advanced Materials, 2015, 27, 6538-6538.                              | 21.0       | 8            |
| 75 | A study on ionic gated MoS2 phototransistors. Science China Information Sciences, 2019, 62, 1.  | 4.3        | 8            |
| 76 | Reliable Nonvolatile Memory Black Phosphorus Ferroelectric Field-Effect Transistors with van der<br>Waals Buffer. ACS Applied Materials & Interfaces, 2019, 11, 42358-42364.                      | 8.0        | 8            |
| 77 | Nanometer-Thick Metastable Zinc Blende γ-MnTe Single-Crystalline Films for High-Performance<br>Ultraviolet and Broadband Photodetectors. ACS Applied Nano Materials, 2020, 3, 12046-12054.        | 5.0        | 8            |
| 78 | High-performance ReS <sub>2</sub> photodetectors enhanced by a ferroelectric field and strain field.<br>RSC Advances, 2022, 12, 4939-4945.  | 3.6        | 8            |
| 79 | Optoelectronics: Highâ€Performance Photovoltaic Detector Based on<br>MoTe <sub>2</sub> /MoS <sub>2</sub> Van der Waals Heterostructure (Small 9/2018). Small, 2018, 14,<br>1870038.               | 10.0       | 7            |
| 80 | Field Effect Transistors: Ferroelectric Negative Capacitance Field Effect Transistor (Adv. Electron.) Tj ETQqO 0 0  | rgBT/Overl | ock 10 Tf 50 |
| 81 | Bio-Separated and Gate-Free 2D MoS2 Biosensor Array for Ultrasensitive Detection of BRCA1.<br>Nanomaterials, 2021, 11, 545.   | 4.1        | 7            |
| 82 | Epitaxial growth and phase evolution of ferroelectric La-doped HfO2 films. Applied Physics Letters, 2022, 120, .  | 3.3        | 7            |
| 83 | Strain-engineered room temperature cavity polariton in ZnO whispering gallery microcavity. Applied Physics Letters, 2020, 116, .  | 3.3        | 6            |
| 84 | Correlation of oxygen vacancy and Jahn–Teller polarons in epitaxial perovskite SrMnO3 ultrathin<br>films: Dielectric spectroscopy investigations. Applied Physics Letters, 2020, 116, .           | 3.3        | 5            |
| 85 | Preparation of La0.67Ca0.23Sr0.1MnO3 thin films with interesting electrical and magnetic properties via pulsed-laser deposition. Science China: Physics, Mechanics and Astronomy, 2017, 60, 1.    | 5.1        | 3            |
| 86 | Multimode Signal Processor Unit Based on the Ambipolar WSe <sub>2</sub> –Cr Schottky Junction.<br>ACS Applied Materials & Interfaces, 2019, 11, 38895-38901.                                      | 8.0        | 3            |
| 87 | Ferroelectric Synapses: A Robust Artificial Synapse Based on Organic Ferroelectric Polymer (Adv.) Tj ETQq1 1 0.   | 784314 rg[ | 3T /Overlock |
| 88 | Exciton Emissions in Bilayer WSe <sub>2</sub> Tuned by the Ferroelectric Polymer. Journal of Physical Chemistry Letters, 2022, 13, 1636-1643.   | 4.6        | 3            |
| 89 | Ultrabroad-Spectrum Photodetectors: Multimechanism Synergistic Photodetectors with Ultrabroad<br>Spectrum Response from 375 nm to 10 Âμm (Adv. Sci. 15/2019). Advanced Science, 2019, 6, 1970089. | 11.2       | 2            |

| 90 | Highâ€Performance Broadband Tungsten Disulfide Photodetector Decorated with Indium Arsenide<br>Nanoislands. Physica Status Solidi (A) Applications and Materials Science, 2020, 217, 2000297. | 1.8 | 2 |
|----|---|-----|---|
|----|---|-----|---|

| #  | Article   | IF   | CITATIONS |
|----|---|------|-----------|
| 91 | Charge-Trap Memory: Eliminating Overerase Behavior by Designing Energy Band in High-Speed<br>Charge-Trap Memory Based on WSe2 (Small 17/2017). Small, 2017, 13, .                               | 10.0 | 0         |
| 92 | Memory Devices: Symmetric Ultrafast Writing and Erasing Speeds in Quasiâ€Nonvolatile Memory via van<br>der Waals Heterostructures (Adv. Mater. 11/2019). Advanced Materials, 2019, 31, 1970081. | 21.0 | 0         |